A Finite Queue Model Analysis of PMRC-based Wireless Sensor Networks

Qiaoqin Li[1], Mei Yang[2], Hongyan Wang[2], Yingtao Jiang[2], Jiazhi Zeng[1]

[1] *College of Computer Science and Technology, University of Electronic Science and Technology, Chengdu, Sichuan, P. R. China*

[2] *Department of Electrical and Computer Engineering, University of Nevada, Las Vegas, NV, 89154*

Emails: [1]{helenli803@163.com, jzzeng@uestc.edu.cn}, [2]{meiyang@egr.unlv.edu, wangh7@unlv.nevada.edu, yingtao@egr.unlv.edu}

Abstract

In our previous work, a highly scalable and fault-tolerant network architecture, the Progressive Multi-hop Rotational Clustered (PMRC) structure, is proposed for constructing large-scale wireless sensor networks. Further, the overlapped scheme is proposed to solve the bottleneck problem in PMRC-based sensor networks. As buffer space is often scarce in sensor nodes, in this paper, we focus on studying the queuing performance of cluster heads in PMRC-based sensor networks. We develop a finite queuing model to analyze the queuing performance of cluster heads for both non-overlapped and overlapped PMRC-based sensor network. The average queue length and average queue delay of cluster head in different layers are derived. To validate the analysis results, simulations have been conducted with different loads for both non-overlapped and overlapped PMRC-based sensor networks. Simulation results match with the analysis results in general and confirm the advantage of selecting two cluster heads over selecting single cluster head in terms of the improved queuing performance.

Key words: wireless sensor network, PMRC, overlap, finite queue model

1. Introduction

Due to their benefits of low cost, rapid deployment, self-organization capability, and cooperative data-processing, wireless sensor networks have been proposed as a practical solution for a wide range of applications [1], such as surveillance and habit monitoring, hazard detection, intelligent agriculture, automation and control, intelligent home, etc. Energy efficiency is treated as the top design objective for wireless sensor networks since each sensor node has limited power to consume. Previous research shows that clustered structure [5] and multi-hop routing [3] achieve better energy efficiency for large-scale sensor networks (as needed in many applications).

In [15], a highly scalable and fault-tolerant network architecture, named as the Progressive Multi-hop Rotational Clustered (PMRC) structure is proposed, which is suitable for the construction of large-scale wireless sensor networks. In the PMRC structure, sensor nodes are partitioned into layers according to their distances to the sink node. A cluster is composed of the nodes located in one layer and the cluster head in the upper layer closer to the sink node. The cluster head is responsible for forwarding data to its upstream layers. A distinguished feature of the PMRC structure is that two cluster heads (the primary cluster head and the secondary cluster head) are selected for each cluster and the two cluster heads rotate to work. The study in [15] shows that by selecting two cluster heads, load balance is achieved and node life time is prolonged.

Similar to other multi-hop structures, the PMRC structure also suffers from the bottleneck problem [12]. In the PMRC structure, the bottleneck problem is reflected on phenomenon that the network life time is limited by the node life time of the cluster heads closer to the sink node. To solve this problem, overlapped neighboring layers is proposed to balance the relay load at the cluster heads for all layers [14]. By overlapping layers, more cluster head candidates are available for each layer and the communication energy in each cluster can be reduced, which ultimately helps prolonging network life time. Simulation results confirm that the overlapped scheme with reasonable overlap ranges achieves significant improvement in network life time.

Besides energy efficiency, quality of service (QoS) requirements [4][13], such as throughput, packet delay, packet loss, should also be satisfied in sensor networks. The buffer space of a sensor node is often limited. Hence, properly choosing the buffer space is also important in designing sensor networks [8].

In the literature, a number of research results on queuing performance analysis for wireless sensor networks have been reported. A typical approach (as adopted in [6][8][9][11]) in queuing analysis for wireless sensor networks is modeling a sensor node as a finite FIFO queue using a continuous time Markov chain assuming sensor nodes alternate between active and sleep modes. The alternation of active/sleep mode may help reduce energy consumption of a sensor node. However, the sleep mode will cause extra delay and packet loss.

In this paper, we focus on the queuing analysis of the PMRC-based wireless sensor networks. Generally all sensor nodes are assumed to be active except the two cluster heads of one cluster may rotate to forward data in

fixed time intervals. Each sensor node is modeled as a M/M/1/N queue model [10]. We then study the network performance in terms of average queue length and average queue delay, and explore the impact of head rotation and the overlapped scheme on these metrics. Through analysis and simulation results, we are giving strong insight into the design parameters that affect the queuing performance.

The rest of the paper is organized as follows. In section 2, the network model and data flow model are described. In Section 3, we develop a finite queue model of cluster heads and analyze the average queue length and the average queue delay of cluster heads at different layers for both non-overlapped and overlapped PMRC structures. In Section 4, simulation results of the two performance metrics are presented and compared with the analysis results. Section 5 concludes the paper.

2. Network Model and Data Flow Model

2.1 Network model

Fig. 1 illustrates an overlapped PMRC structure [14], Without loss of generality, we assume that the sensor nodes are distributed uniformly with density ρ in a circular area and the sink node is located at the center of the area. The circular area can be partitioned into a set of sub-areas, each one composed of the clusters formed in consecutive layers. Each sub-area can be represented as a fan shape with angle θ (see Fig. 1).

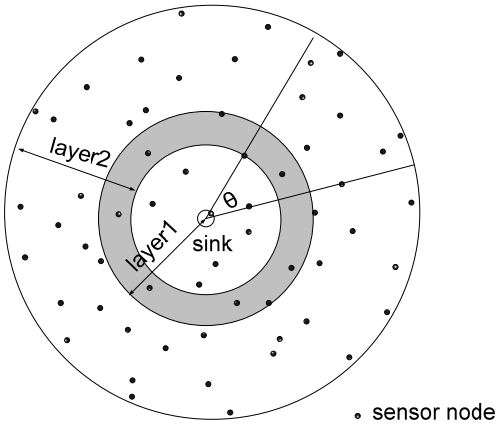

Figure 1 Overlapped layers in a PMRC-based sensor network [14].

As shown in the figure, layer 1 occupies a circular area and layer 2 is shown in a ring shape. The grey area indicates the overlapped area of layer 1 and layer 2. Layer 1 is considered as the *inner layer* of layer 2 and layer 2 is considered as the *outer layer* of layer 1. Note that the sensor nodes in the grey area still belong to layer 1 while they are the candidate cluster heads for clusters in layer 2. Particularly, the sink node is the cluster head of the single cluster formed in layer 1. The non-overlapped PMRC structure can be considered as a special case of the overlapped PMRC structure with no overlapped area between adjacent layers.

2.2 Data flow model

Assume that all nodes in the circular area are active in transmission and a portion of these nodes are active in sensing. We assume the sensed data are organized into packets with a variable size following exponential distribution. The data generating process at each sensor node follows a Poisson process, and all the sensing events in the wireless network occur independently. Each sensing node transmits its sensed data to its cluster head. Each cluster head then sends all sensed data within its cluster and relays data coming from the cluster head in its outer layer to the cluster head in its inner layer.

In the PMRC-based sensor network, sensor nodes belonging to the same cluster compete on the common channel for data transmission. According to [8], in a contention-based sensor network, the relay packets from the outer layer can be also assumed as a Poisson process as long the length of contention window is much smaller than the interval of packets. Hence, the arrival process at the cluster head of each layer can also be considered as a Poisson process following the superposition property of Poisson process. We also assume that there is no data aggregation at all layers.

3. Analysis

The following notations will be used in our analysis.

R: diameter of the circular area of the wireless sensor network.

n: maximum number of layers in the circular area.

r: transmission and sensing range of the sensor nodes.

ρ: sensor node density in the circular area.

α: ratio of the number of sensing nodes to the total number of nodes, $0 \le \alpha \le 1$.

θ: angle of the fan shape in overlapped PMRC structure.

θ': angle of the fan shape in non-overlapped PMRC structure.

r_i: range of the ring shape in layer i for overlapped PMRC structure, where $r_1=r$.

r_i': range of the ring shape in layer i for non-overlapped PMRC structure, where $r_1'=r$.

x_i: range of the overlapped area of layer i and layer i+1.

λ_0: data generation rate of sensed data at each node.

λ_i: data arrival rate at cluster head in layer i for overlapped PMRC structure.

λ_i': data arrival rate at cluster head in layer i for non-overlapped PMRC structure.

μ: data transmission rate of a sensor node.

μ_i: service rate of cluster head in layer i for overlapped PMRC structure.

μ_i': service rate of cluster head in layer i for non-overlapped PMRC structure.

K_i: buffer size at cluster head in layer i.

N_i: number of neighboring sensor nodes of a cluster head in layer i for overlapped PMRC structure.

N_i': number of neighboring sensor nodes of a cluster head in layer i for non-overlapped PMRC structure.

3.1 Node queue model

For a cluster head in layer i, with the Poisson arrival process of rate λ_i, the exponentially distributed service of rate μ_i, buffer size K_i, it can be modeled as a M/M/1/K_i queue system, as shown in Fig. 2.

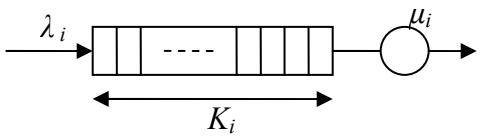

Figure 2 Queuing model of cluster heads in layer *i*.

We observe that the arrival rate to the overlapped PMRC structure and non-overlapped PMRC structure are different. In the following, we will show the derivation of λ_i for overlapped PMRC structure followed by the derivation of λ_i' for non-overlapped PMRC structure.

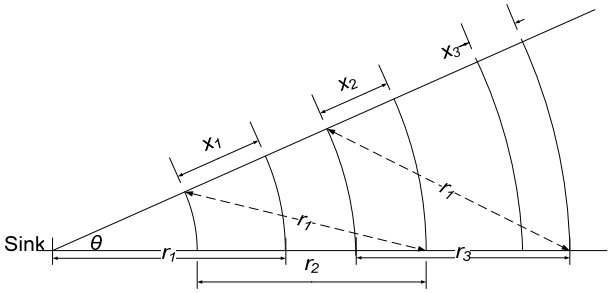

Figure 3 Top view of three overlapped layers [14].

We first consider the arrival rate of a cluster head in the overlapped area between layer 1 and layer 2. Consider the fan shape with angle θ which corresponds to one cluster range in each layer. From Fig. 3, the arrival rate to the cluster head in layer 1 can be derived as

$$\lambda_1(\theta)= \lambda_0\rho\alpha(R^2 - r_1^2)\theta/2 = \lambda_0\rho\alpha\theta(R^2 - r_1^2)/2,$$

where $\theta(R^2 - r_1^2)/2$ gives the area outside layer 1.

For simplicity, we normalize the value of r_1 as 1. Assume $R = n*r_1$, then we get $R=n$. Thus $\lambda_1(\theta)$ can be derived as:

$$\lambda_1(\theta) = \lambda_0\rho\alpha\theta(n^2 - 1)/2 \quad (1)$$

Next, we derive λ_2 as follows. To find out the overlapped area of layer 2 and layer 3, we need calculate r_2, which can be obtained by geometry relations as:

$$r_2(x_1,\theta) = \sqrt{1-(1-x_1)^2\sin^2\theta} - (1-x_1)(1-\cos\theta) \quad (2)$$

We then get

$$\lambda_2(x_1,\theta) = \lambda_0\rho\alpha\theta(n^2 - (1+r_2-x_1)^2)/2 \quad (3)$$

We then derive r_3 and λ_3 as follows.

$$r_3(x_1,x_2,\theta) = \sqrt{1-(1+r_2-x_1-x_2)^2\sin^2\theta} - (1+r_2-x_1-x_2)(1-\cos\theta) \quad (4)$$

$$\lambda_3(x_1,x_2,\theta) = \lambda_0\rho\alpha\theta(n^2 - (1+r_2+r_3-x_1-x_2)^2)/2 \quad (5)$$

Generally, we have,

$$r_n(x_1,x_2,...,x_{n-1},\theta) = \sqrt{1-(\sum_{i=1}^{n-1}(r_i-x_i))^2\sin^2\theta} - (\sum_{i=1}^{n-1}(r_i-x_i))(1-\cos\theta) \quad (6)$$

$$\lambda_n(x_1,x_2,...,x_{n-1},\theta) = \lambda_0\rho\alpha\theta(n^2 - (\sum_{i=1}^{n-1}(r_i-x_i)+r_n)^2)/2 \quad (7)$$

According to the analysis in [14], θ is chosen at 27º for overlapped PMRC structure.

The arrival rate at the cluster heads in each layer in no-overlapped PMRC structure can be derived as follows.

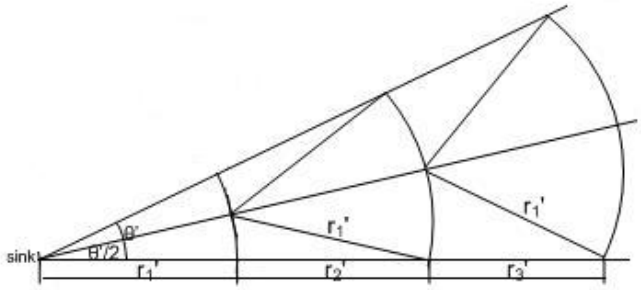

Figure 4 Top view of three non-overlapped layers.

Figure 4 illustrates the layer relation in non-overlapped PMRC structure. From Fig. 4, we can derive that

$$\lambda_1'(\theta') = \lambda_0\rho\alpha\theta'(n^2 - 1)/2 \quad (8)$$

According to geometry relations, r_2' is calculated as:

$$r_2'(\theta') = 1 - (2\sin\frac{\theta'}{4})^2 \quad (9)$$

We then get

$$\lambda_2'(\theta') = \lambda_0\rho\alpha\theta'(n^2 - (1+r_2')^2)/2 \quad (10)$$

Following similar way, we can derive r_i' and λ_i' for i>2. θ' is typically set slightly larger than θ as the cluster size generated in the non-overlapped PMRC structure tends to be larger than that in the overlapped PMRC structure.

For both overlapped and non-overlapped PMRC structure, the service rate can be derived in the same way. Assume that sensor nodes in the same cluster compete on the common channel for data transmission through random back-off scheme. The back-off time is a random number with a discrete uniform distributed between 0 and CW-1, where CW is the contention window size. Taking the example of overlapped PMRC structure, the probability of the cluster head in layer i wins the channel can be derived as follows.

$$P_{win} = (1-\frac{1}{CW})^{N_i-1} \quad (11)$$

where N_i is the number of neighboring nodes of the cluster head in layer i competing for the channel.

Then, we have the rate of service time of cluster head in layer *i*.

$$\mu_i = \mu P_{win} = \mu(1-\frac{1}{CW})^{N_i-1} \quad (12)$$

3.2 Queuing performance metrics

In our study, we consider two queuing performance metrics, the average queue length at layer *i* and the average queue delay at layer *i*.

To derive the average queue length at layer *i*, we derive the steady-state queue length distribution of cluster head in layer *i* first. Denote $P_j(i)$ as the probability that there are *j* data packets in the buffer of a cluster head in layer *i*. Then $P_j(i)$ can be derived as:

$$P_j(i) = \frac{1-\rho_i}{1-\rho_i^{K_i+1}}\rho_i^j, \qquad 0 \le j \le K_j \quad (13)$$

where $\rho_i = \frac{\lambda_i}{\mu_i}$.

Then the average queue length (i.e., the average number of data packets in the queue of the cluster head) at layer *i* can be calculated as:

$$E[n_i] = \sum_{j=1}^{K_i} jP_j(i) = \frac{\rho_i}{1-\rho_i} - \frac{(K_i+1)\rho_i^{K_i+1}}{1-\rho_i^{K_i+1}} \quad (14)$$

According to Little's Law [10], the average queue delay at layer *i* can be calculated as:

$$E[d_i] = \frac{E[n_i]}{\lambda_i} \quad (15)$$

4. Performance Evaluation

To validate our analysis, simulations of both overlapped and non-overlapped PMRC structure based on the simulation models [14][15] developed on OPNET Modeler network simulator have been conducted. The wireless channel allocation model provided in OPNET is used in our simulations.

4.1 Simulation settings

In the simulations, we assume a 200*m*x200*m* geographical area covered by a sensor network with the sink node located at the center. All the sensor nodes are uniformly distributed in the network. Tab. 1 lists some basic parameters used in our simulations.

Table 1. Basic simulation parameters.

Parameter	Value
Sensor field area	200*m* x 200*m*
Node number (*N*)	400
Radio transmission range (R_t)	*40m*
Initial energy per node	2*J*
Buffer size	50 packets
Mean packet size	500 bytes
Channel bandwidth	1 *Mbps*
Transmission speed at each node (μ)	9600 *bps*
Data generation rate (λ_0)	{0.3, 0.36, 0.42, 0.48, 0.54, 0.59} *pkt/s*
Simulation time	Until the first node death

The following performance metrics are collected:

Average queue length: the average queue length is averaged from the time when the first packet arrives at the queue until the simulation ends.

Average queue delay: the queue delay of a packet is the difference of the time when the packet arrives at the queue and the time when the packet leaves the queue.

In the following, we present the simulation results of the two performance metrics for two sets of different configuration scenarios: 1) Non-overlapped PMRC, and transmission range of 40*m*; 2) Overlapped PMRC, and transmission range of 40*m*. For each scenario, we simulate two types of cluster head selection strategies: single-head (represented as 'S' in all figures) and double-head (the primary cluster head (PCH) is represented as "DP" and the secondary cluster (SCH) head is represented as "DB" in all figures). In double-head selection, the PCH and the SCH for a cluster rotates to work in 10 seconds interval. The analysis results in Section 3 (which have been adjusted to fit for the square area) are represented as "A" in all figures. For all simulations, the same number of nodes evenly distributed in the whole area are selected to sense the data and generate the packets.

4.2 Performance of non-overlapped PMRC structure

Figs. 5-6 present the averaged performance metrics of cluster heads locating in layers 1 and 2 for the non-overlapped PMRC structure. The performance metrics for cluster heads in other layers are omitted here for clearness reason.

Fig. 5 shows that the average queue length of cluster heads at different layers vs. the data generation rate at each sending node (i.e., λ_0) with transmission range of 40*m*. It shows that the average queue length of cluster heads at one layer increases with the increase of λ_0. Generally, the average queue length of one type of cluster heads in layer 1 is larger than that of the same type of cluster heads in layer 2. This is consistent with our intuition that the average traffic load to cluster heads closer to the sink node is higher than those farther from the sink node.

Fig. 5 also shows that under the same set of sensing nodes, the average queue length of single cluster head is larger than that of the primary/secondary cluster head at the same layer. This is because that with dual cluster heads, the two heads rotate to receive data packets from their outer layers. This reduces the queue length of each head. The average queue length of the PCH is larger than that of the SCH in the same layer. This is because the SCH may not cover all the nodes in its cluster according to SCH selection algorithm [15].

In Fig. 5, the analysis result of the average queue length for cluster heads in layer 2 is close to that of the simulation result with single cluster head while the analyzed result for cluster heads in layer 1 is different from the corresponding simulation result. We expect that

this difference will be mitigated by averaging the simulation results of different sets of sending nodes.

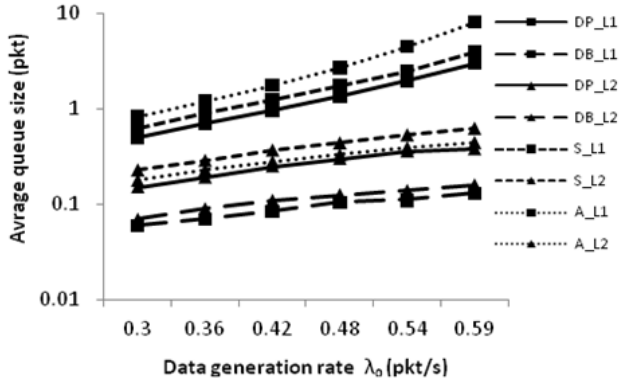

Figure 5 Average queue length vs. λ_0 for non-overlapped PMRC structure.

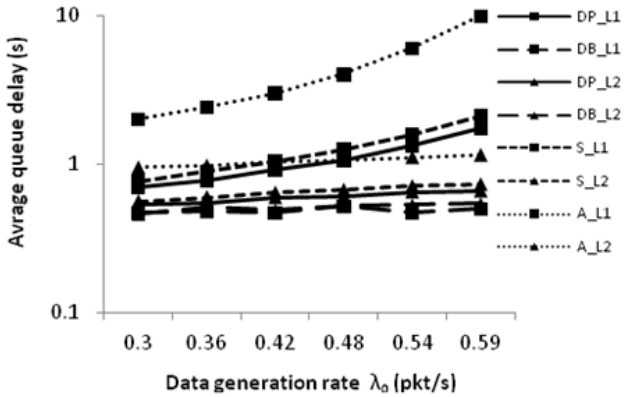

Figure 6 Average queue delay vs. λ_0 for non-overlapped PMRC structure.

Fig. 6 shows that the average queue delay of cluster heads at one layer increases with the increase of λ_0. The trend is similar to the queue length. Generally, the average queue length of one type of cluster heads in layer 1 is larger than that of the same type of cluster heads in layer 2. This is because that the larger the queue length, the longer waiting time of a packet in the queue. Similar to Fig. 5, under the same set of sensing nodes, the average queue delay of single cluster head is larger than that of the primary/secondary cluster head at the same layer.

In Fig. 6, the analysis result of the average queue delay is generally larger than the corresponding simulation result. It is expected that the difference between the simulation results and analyzed results will be mitigated by averaging the simulation results of different sets of sending nodes.

4.3 Performance of overlapped PMRC structure

Figs. 7-8 present the averaged performance metrics of cluster heads locating in layers 1 and 2 for overlapped PMRC structure. In overlapped PMRC structure, with the same transmission range, more layers are created than non-overlapped PMRC structure. For clearness purpose, The performance metrics for cluster heads in other layers are omitted here. Comparing Figs. 5 and 7, the average queue length of single head at one layer for overlapped PMRC structure is lower than the corresponding result for non-overlapped PMRC structure. And it is apparent that the queue length of the primary cluster head in one layer (for example DP_L1) for overlapped PMRC is much smaller than that of its corresponding result for non-overlapped PMRC. This is the due to the fact that with overlapped layers, more candidate cluster heads are available and the coverage of secondary cluster heads is improved. This helps balance the traffic load between the primary cluster head and the secondary cluster head at the same layer. Similar results are reflected by comparing Figs. 6 and 8.

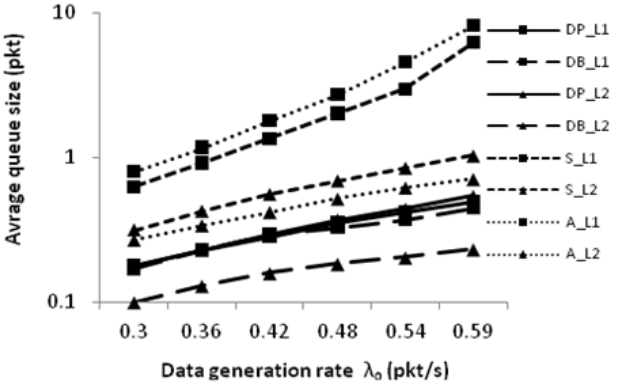

Figure 7 Average queue length vs. λ_0 for overlapped PMRC structure.

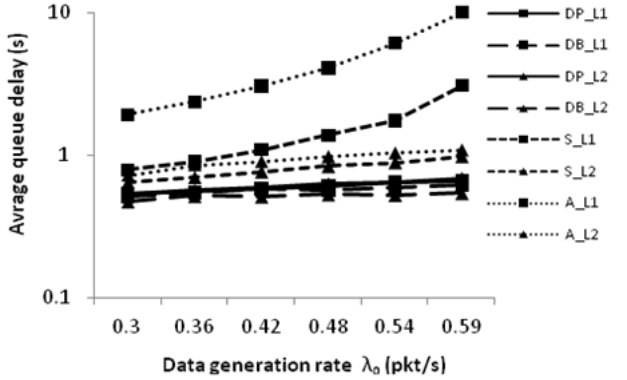

Figure 8 Average queue delay vs. λ_0 for overlapped PMRC structure.

An abnormity in these figures is that the average queue length for cluster heads in inner layers (e.g., DP_L1) may not always larger than that of the cluster heads in outer layers (e.g., DP_L2). This can be explained that the coverage of SCH in outer layers may not be as good as in inner layers. We can deduce that the average queue length of cluster heads in inner layers will not increase definitely.

The analysis results of the average queue length (from Eqn. (14)) and average queue delay (from Eqn. (15)) of cluster heads at layers 1 and 2 are also shown on Figs. 7 and 8, respectively. Compared with Figs. 5 and 6, we can

see that the analyzed results are closer to the simulation results. This is because that the number of clusters generated in overlapped PMRC at each layer is typically more than that in non-overlapped PMRC, which helps averaging the simulation result.

5. Conclusion and Future Works

In this paper, we develop a finite queuing model for analyzing the queuing performance for cluster heads in both non-overlapped and overlapped PMRC-based wireless sensor network. The simulation results of the average queue length and the average queue delay match the analysis results in general trend. The simulation results also confirm that the scenarios with double cluster heads outperform the scenarios with single head in terms of the two performance metrics. Compared with non-overlapped PMRC, overlapped PMRC improves the queuing performance of the scenarios of double cluster heads.

The presented analysis provides a guideline in deciding the buffer size of sensor nodes in PMRC-based sensor networks. Future work includes the analysis of other network performance metrics and their relations with the energy consumption at sensor nodes.

References

[1] I. F. Akyildiz, W. Su, Y. Sankarasubramaniam, and E. Cayirci, "A survey on sensor networks," *IEEE Commu. Mag.*, pp. 102-114, Aug. 2002.

[2] C. F. Chiasserini, M. Garetto, "Modeling the performance of wireless sensor networks," *IEEE INFOCOM*, 2004, vol. 1, pp. 7-11.

[3] J. Ding, K. Sivalingam, R. Kashyapa and L.J. Chuan, "A multi-layered architecture and protocols for large-scale wireless sensor networks," *Proc. IEEE SVTC*, 2003, pp. 1443-1447.

[4] A. Fallahi, E. Hossain, and A. S. Alfa, "QoS and energy trade off in distributed energy-limited mesh/relay networks: a queuing analysis," *IEEE Trans. Parallel and Distributed Systems,* vol.17, no.6, pp. 576-592, 2006.

[5] W. Heinzelman, A. Chandrakasan, and H. Balakrishnan, "An application-specific protocol architecture for wireless microsensor networks," *IEEE Trans. Wireless Communications*, vol. 1, no. 4, pp. 660-670, 2002.

[6] J. M. Liu, T. Lee, "A framework for performance modeling of wireless sensor networks," *Proc. ICC*, 2005, vol. 2, no. 2, pp. 1075-1081.

[7] C Lu, B.M. Blum, T.F. Abdelzaher, J.A. Stankovic and T. He, "RAP: a real-time communication architecture for large-scale wireless sensor networks," *Proc. 8th IEEE RTAS*, 2002, pp. 55-66.

[8] J. Luo, L. Jiang, and C. He, "Finite queuing model analysis for energy and QoS tradeoff in contention-based wireless sensor networks," *Proc. ICC*, 2007, pp. 3901-3906.

[9] S. Moon, S. Lee and H. Cha, "A congestion control technique for the near-sink nodes in wireless sensor networks," *Proc. UIC*, 2006, LNCS 4159, pp.488-497.

[10] T. G. Robertazzi, *Computer Networks and Systems: Queueing Theory and Performance Evaluation*, 3rd Edition, Springer-Verlag New York, New York, NY, 2000.

[11] T. Shu, M. Krunz, and S. Vrudhula, "Power balanced coverage-time optimization for clustered wireless sensor networks," *Proc. Int'l Symp. Mobile Ad Hoc Networking & Computing*,2005, pp. 111-120.

[12] S. Soro and W. Heinzelman, "Prolonging the lifetime of wireless sensor networks via unequal clustering", *Proc. 19th IEEE Int'l Parallel and Distributed Processing Symp. (IPDPS)*, 2005.

[13] S. Tang and W. Li, "QoS supporting and optimal energy allocation for a cluster based wireless sensor network," *Computer Communication*, vol. 29, pp. 2569-2677, 2006.

[14] H. Wang, M. Yang, Y. Jiang, S. Wang, L. Gewali, "Overlapped layers for prolonging network lifetime in multi-hop wireless sensor networks," to be presented on ITNG, 2008, Las Vegas, NV.

[15] M. Yang, S. Wang, A. Abdelal, Y. Jiang, and Y. Kim, "An improved multi-layered architecture and its rotational scheme for large-scale wireless sensor networks," *Proc. IEEE CCNC*, 2007, pp. 855-859.